

New-generation simultaneous shooting sparse OBN survey and FWI delineate deep subsalt structures in the Greater Mars-Ursa area

Henrik Roende¹, Dan Chaikin¹, Yi Huang¹, and Konstantin N. Kudin²<https://doi.org/10.1190/tle39110828.1>

Abstract

The U.S. Gulf of Mexico (GoM) geology is well known for prolific structural hydrocarbon traps created by salt tectonics. In many areas, these structures lie below salt overhangs or thick canopies, requiring advanced seismic imaging to identify prospects and plan exploration wells. Ever-evolving geophysical technologies, such as 3D seismic, wide azimuth, multiwide azimuth, coil, and ocean-bottom node (OBN) acquisition designs, have unlocked the image for some of these structures over the past three decades. Recently, automatic velocity model building methods, particularly full-waveform inversion (FWI), introduced another step change in the subsalt image quality and refocused the acquisition methods on the need to acquire long-offset data. To make such a long-offset program affordable, a new survey geometry was set up with sparse OBN nodes and simultaneous shooting. The actual survey was acquired in 2019 and fully processed within 15 months from the end of the acquisition. Offsets up to 65 km were recorded, enabling FWI velocity updates down to 15 km depth. To provide the reader with a glimpse of the geologic insight that the new technology enabled, we report a few examples of deep geology revealed by this survey in a hydrocarbon- and seismic-data-rich area of the GoM — the Greater Mars-Ursa Basin.

Introduction

Exploration in the Greater Mars-Ursa area was opened with a 1984 well, which was drilled on top of the Venus salt body (Venus well, MC852 Getty no. 1) (Figure 1). The well encountered a 4 ft 29% porosity sand that was filled with light oil. Follow-up wells were significantly more successful and discovered multiple billions of barrels of hydrocarbons in place. For a detailed historical account of oil industry activities in the area, see Priest (2019).

Today, Shell, together with different coowners, operates several major fields in the Greater Mars-Ursa area. They support three producing tension leg platforms, including Mars, Ursa, and Olympus, with a fourth currently being built (Vito). Over the past 30 years, many proprietary and multiclient streamer surveys were acquired in the area, designed to image the numerous prolific reservoirs. Among the most recent surveys relevant to the current work are two wide-azimuth (WAZ) surveys shot in the area in 2009 (Freedom WAZ) and 2012 (orthogonal Patriot WAZ).

Additionally, Shell development and production teams have acquired patches of ocean-bottom node (OBN) data on a 400 × 400 m hexagonal node grid covering individual fields. Over time, these 3D and 4D OBN surveys yielded a sizable blanket of dense OBN coverage, providing full-azimuth (FAZ) data at near and mid offsets.

Despite such an abundance of seismic data, some parts of the basin were still found to be poorly imaged, even more so in the deeper prospective section. For proper focusing, velocity analysis must accurately determine salt/sediment interfaces, intrasalt velocity variations, lateral variations within Miocene structures, localized velocity inversions from overpressure, and proper placement of the velocity increase at the base of the Miocene section. The complex salt-tectonic-related structures, which generate near-vertical dips and raft older stratigraphy into shallow younger sections, become more challenging to resolve under the salt canopy. This complexity

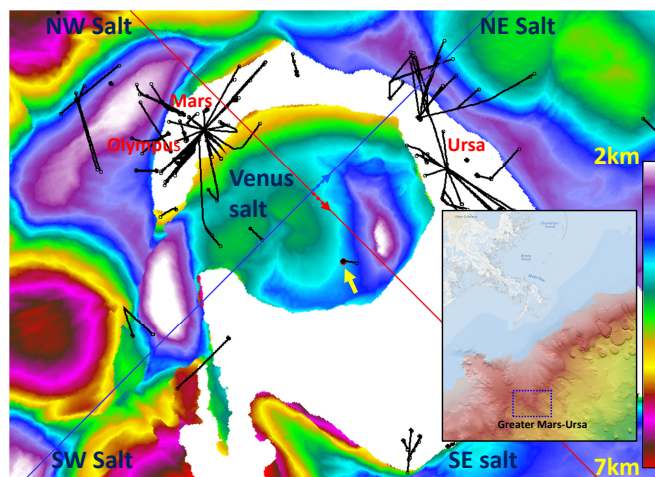


Figure 1. Top-of-salt map in the Greater Mars-Ursa area, centered on the Venus salt body, with a selection of publicly released wells. The first well in the area, MC852 Getty no. 1, is highlighted by the yellow arrow at the south side of the Venus salt body. The red inline and blue crossline with respective arrows indicate the location and direction (left to right) of the seismic lines in Figures 3 and 4. For scale, the areal size of the Venus salt body is approximately 10 km in diameter. The inset bathymetry map shows the location of the Greater Mars-Ursa area relative to the New Orleans coastline. Courtesy of the Bureau of Ocean Energy Management.

¹TGS, Houston, Texas, USA. E-mail: daniel.chaikin@tgs.com; henrik.roende@tgs.com; yi.huang@tgs.com.

²Shell Exploration and Production Company, Houston, Texas, USA. E-mail: konstantin.kudin@gmail.com.

drove the increased sophistication of velocity model building techniques prior to full-waveform inversion (FWI) technology, but proper focusing remained elusive. For example, streamer-based traveltimes tomography was unable to resolve velocities in more structurally complicated subcanopy areas due to single arrival assumptions and lack of offset or event resolution in the gathers.

With the specific intent of unlocking deeper geologic complexities under the salt canopy via FWI, a new generation of sparse OBN data were acquired in the area in 2019. This multiclient Amendment survey was designed to record very long-offset data of no less than 20 km and to underpin the FWI velocity model building approach. The aspiration was to use the higher-fidelity FWI velocity model to upgrade the seismic image for the shallower reservoirs by adding offsets for imaging up to 20 km and offsets for FWI up to 65 km.

To demonstrate the possibilities enabled by the new generation of seismic technology, we compare newly acquired OBN data to earlier WAZ data sets. We highlight the benefits of the new velocity model rebuilt via FWI by comparisons with prior generation velocity model migrations. To thoroughly understand imaging uplift due to different elements of the new technology, we focus on representative seismic cross sections of a challenging structure under Venus salt in the Mars-Ursa area. We also comment on newly observed geologic features revealed by the survey.

Survey acquisition and processing

The survey was designed to record offsets that could capture diving waves to the Louann level, which in this area sits at approximately 12 km depth below the sea surface (Van Avendonk et al., 2015). Extensive modeling (Huang et al., 2019) indicated that offsets up to 35–40 km were needed. A sparse-node grid of 1 × 1 km with 3000 nodes would cover the area of 2700 km² (Dellinger et al., 2016; Roende et al., 2019).

The survey was acquired from April to August 2019, with a duration of 122 days. All nodes were recovered and had a failure rate of 0.4% (a total of 12 nodes). The survey had zero recordable incidents but was challenged with 108 close passes for three dual-source boats. The source density was set to 50 × 100 m, with a shot halo of 20 km outside the receiver patch. The shot spacing was designed to ensure that 1.6 million shots could be fired within the duration of the battery life of the receivers. The relatively high shot density was intended to facilitate deblending. Low frequencies down to 1.6 Hz were usable on the offsets up to 15 km. For a more detailed description of the numerous geophysical details for the survey, we refer the reader to Roende et al. (2020).

The dynamic matching FWI (Mao et al., 2020) was run using a smoothed starting model from the most recent underlying dual-WAZ velocity model building project (2016 vintage). The data were input to FWI with minor processing steps. Specifically, the FWI input was zero phased to ensure that there were no subsequent timing shifts between the derived FWI velocity model and the final zero-phase time data used as the input to migrations. To make the input data amenable to the existing algorithms that are optimized for single-shot data, deblending was performed using a hybrid deblending approach. This included rank-minimization-based denoising for signal extraction and local window f - k domain inversion-based deblending for residual deblending (Figure 2). On the time slice, the strong amplitudes of direct arrivals are readily observable. On the outboard side, we notice the refracted energy and can see the reflected signal inside the first arrival.

Imaging improvements

The imaging uplift achieved in this project is due to the combination of two elements. First, OBN data provide improved illumination due to the uniform FAZs and long offsets. Second, a higher-fidelity velocity model is created by applying FWI to the long-offset OBN data. We present two detailed panels of the OBN/WAZ data migrated with a mature previous generation velocity model derived from dual-WAZ data (2016 vintage) (Figure 3) and the same OBN/WAZ data migrated with a new-generation FWI velocity model (2020 vintage) (Figure 4). By cross-comparing the panels, we can determine contributions of the FAZ and higher-fidelity FWI velocity model to overall

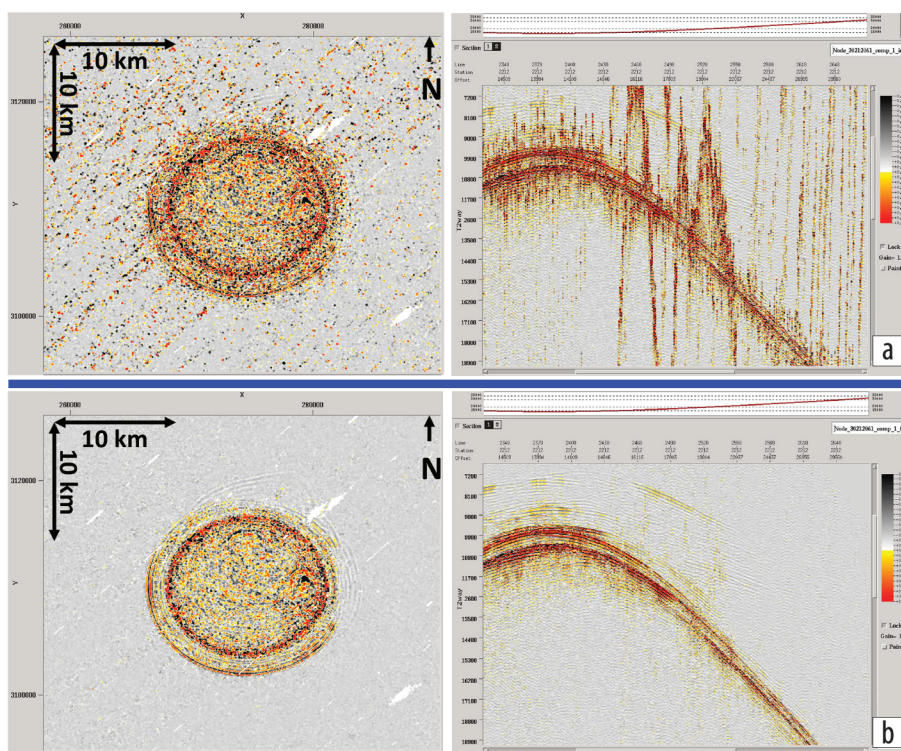


Figure 2. A geophone record from the survey. (a) Acquired data, time slice at 5000 ms (left), and offset data (right). (b) The same displays in (a) after deblending.

image improvement. Figure 3b shows that OBN input migration using the 2016 velocity was able to reveal additional deeper structures and steep dips that were not observed in the dual-WAZ input in Figure 3a. This is most notable under the Venus and southeast salt bodies in Figure 3b (magenta arrow). However, interpretability of the OBN image is still poor due to velocity errors, resulting in a lack of proper focusing and significant mispositioning errors. Using Figure 4 migrations as the ground truth, we can estimate these lateral positioning errors to be on the order of 100–200 m for steep horizons under the Venus salt. Overall, one could argue that the OBN data with a previous generation velocity model were not game changers in this area of mature seismic data quality with two orthogonal WAZ surveys.

On the other hand, using the large offsets and frequency range of OBN data in FWI velocity model building fully reveals the power of the new generation of acquisition and processing technology (Figure 4). The shallow gas clouds, notable in Figure 4c for the Venus and southwest salt bodies, have become commonplace for many applications of FWI technology at shallower depths and could be seen in the past with shorter-offset streamer data FWI updates. The higher-fidelity FWI intrasalt velocities that heal reflector discontinuities below salt have also been reported for existing fields under development, such as Mad Dog (Nolte et al., 2019) and Atlantis (Shen et al., 2017; Mei et al., 2019). Due to the depths, longer-offset OBN data were essential to adjust deeper intrasalt velocities and improve focusing in those projects. In this paper, we provide an example of FWI updates, all the way down to the sedimentary basement at approximately 15 km depth (blue arrow in Figure 4c).

Comparing Figures 3c and 4c, FWI has significantly altered velocities throughout the basin and under the salt canopy. Velocity trends are modified, and the velocities below the Miocene section are sped up (yellow to red velocity colors). These updates are not dip dependent and are observed for both horizontal and nearly vertical beds. Comparing the migrated seismic data in Figures 3 and 4 shows that FWI led to improved focusing and healing of event breaks under the salt canopy. The basement reflector at approximately 15 km depth is readily trackable on the new FWI data. Although not perfectly focused everywhere yet, it signifies an important improvement compared to Figure 3b, where

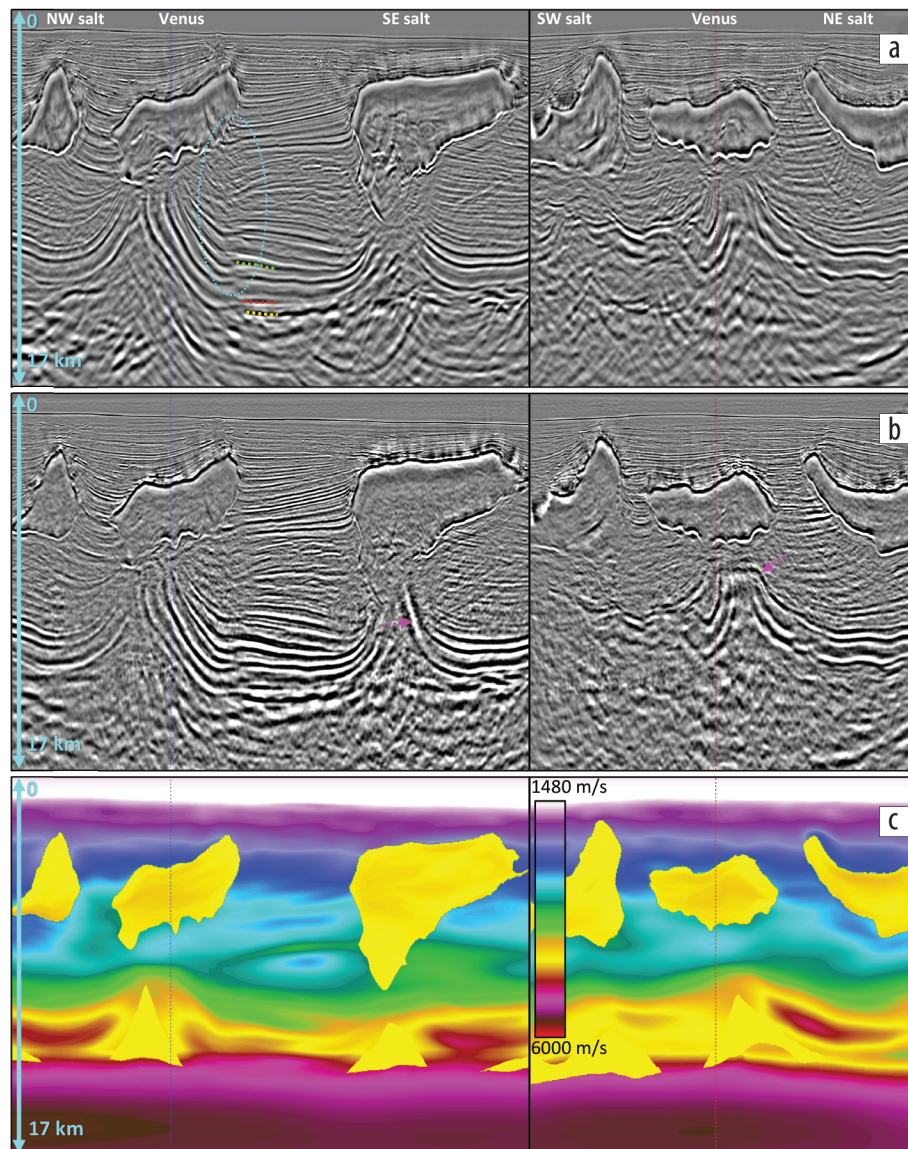


Figure 3. Data migrated with the 2016 velocity model and the respective velocity model itself. (a) Dual-WAZ reverse time migration (RTM). (b) OBN RTM. (c) 2016 model derived from dual-WAZ tomography and manual salt modeling. In (a), Oligocene is marked with a green dotted line, Louann with a red dotted line, and basement with a yellow dotted line. A cyan oval highlights the reflectors discontinuity under the Venus salt edge. In (b), magenta arrows indicate OBN imaging improvements versus WAZ.

the reflector is missing in many locations. Focusing of the basement reflector serves as a conclusive test of whether the average velocities of the entire geologic section above are quantitatively correct.

Finally, the quality of the final velocity model in Figure 4c indicates that the overall performance of the FWI algorithm used in this work appears comparable to the results described in Zhang et al. (2018).

Impact of new-generation seismic data on our understanding of deep geology

The main challenge in focusing the image and delineating the structures in this area is the presence of an extensive salt canopy embedded within younger sands and shales. Imaging is dependent on accurate velocity within and under the salt, which

is difficult to determine through traveltome tomography based on gather analysis. Subsalt velocities vary according to structure, geologic age, and overpressure distribution. The Miocene-Oligocene boundary (green dotted line in Figures 3a and 4a) is characterized by a velocity speedup that persists through the Mesozoic section to the in-situ Louann (red dotted line). The correct location of this velocity kick is critical to building accurate velocity models for areas where such a section is located at fairly shallow depths (see the structure under the Venus salt in Figure 4c). Imaging of this subsalt structure is further obscured by geophysical complexity of the shallower salt canopy itself, within which the salt velocities may deviate significantly from pure salt velocities. The new generation of data reveal and refine many of these challenging features. Laterally, velocity trends are more accurate with greater detail, such that major structure breaks observed with the 2016 velocity model are healed when using the 2020 FWI velocity field. See the prominent reflector discontinuities within the cyan ovals under the southeast side of the Venus salt body, which are healed from Figures 3a to 4a. Migration of the OBN and WAZ data with the FWI velocity greatly improves interpretability of the prominent Oligocene-Mesozoic megaflaps. The older and faster section has risen from its normal stratigraphic depth all the way to the canopy level along the salt flanks, as indicated by the yellow arrows in Figure 4a.

As has been observed in the past, the velocities within seemingly uniform salt bodies may deviate by several hundreds of meters per second from the commonly assumed pure salt velocities (4480 m/s), thus causing image discontinuities below the salt overhangs. For example, for the salt body near Kepler Field, Elebiju et al. (2016) determine that slower salt velocities helped heal a reservoir reflector discontinuity at the edge of the salt, with subsequent wells confirming the validity of the intrasalt velocity slowdown assumption. Venus salt looks to be another peculiar salt body. Various prior dirty salt velocity model building approaches (such as traveltome tomography in the 2016 velocity model) (Figure 5a) failed to properly capture details of the velocity field variability within the salt body. These errors led to artificial reflector discontinuities on the migrated image (cyan oval in Figure 3a). FWI with long-offset OBN data

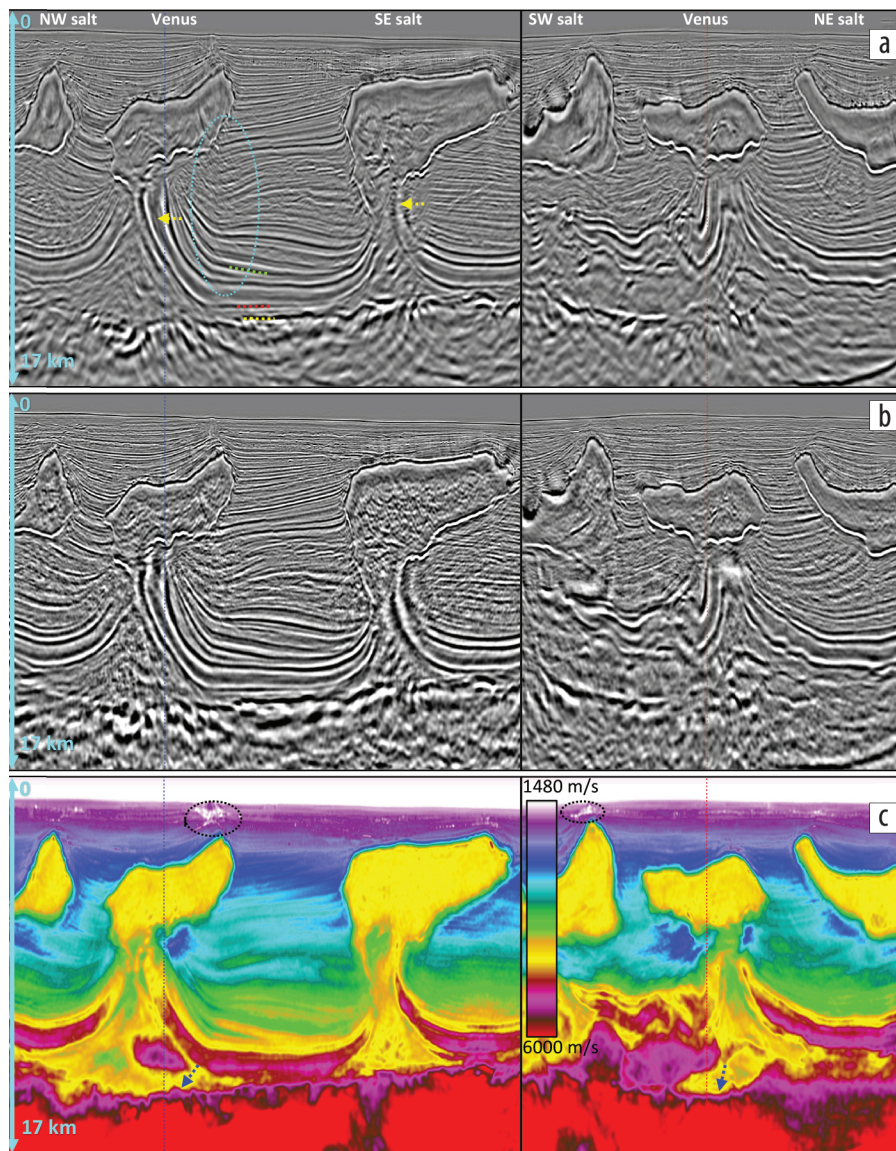


Figure 4. Data migrated with the 2020 FWI velocity model and the respective velocity model itself. (a) Dual-WAZ RTM. (b) OBN RTM. (c) 2020 model derived via FWI using long-offset OBN data. In (a), Oligocene is marked with a green dotted line, Louann with a red dotted line, and basement with a yellow dotted line. A cyan oval highlights the healed reflectors under the Venus salt edge. Yellow arrows point to megaflaps. In (c), black ovals highlight shallow gas clouds, and blue arrows indicate the velocity update down to 15 km.

accurately resolves these important intrasalt details. By comparing the depth slices and traverses on Figures 5a and 5b, we observe that FWI largely inverted intrasalt velocity slow and fast zones within the Venus salt compared to the 2016 model. Physically meaningful spatially dependent velocity slowdowns within the salt heal reflector discontinuities under the salt edge (cyan oval in Figure 4a). Notably, FWI revealed that intrasalt velocity slowdowns are highly nonuniform and do not have enough obvious intrasalt reflectors to help localize such slowdowns by other means. The base salt reflector is also better focused, as is the entire subsalt section, and the underlying break in the prominent Oligocene horizon is healed.

The velocities of the Mesozoic megaflaps are dramatically increased, correcting their position. This is one of the more striking

imaging improvements (yellow arrows in Figure 4a). Pre-FWI conventional traveltime tomography methods were unable to resolve these nearly vertical fast Mesozoic layers, typically resulting in large velocity errors that mispositioned and unfocused the structures. Finally, the higher-fidelity FWI velocities within the entire sediment section yield a mostly flat basement reflector at approximately 15 km depth in large sections of the seismic line (Figure 4b).

Conclusions

The seismic data examples presented in this paper demonstrate that the new generation of seismic acquisition and processing provides a step change in subsalt image quality. With the existing previous-generation velocity models, long-offset OBN data may provide a modest uplift to imaging of the deep structures due to

its uniform FAZ illumination and long offsets. However, the bulk of the uplift can only be achieved when very long-offset OBN data are used per the original intent in order to rebuild the velocity model via FWI. Furthermore, thanks to the focusing improvements enabled by higher-fidelity FWI velocity, the existing dual-WAZ data image is significantly improved as well.

The deep geology revealed by the current survey is rather spectacular and will keep structural geologists, salt tectonics experts, oil prospectors, and other interpreters busy for quite some time. While we only discussed the results from the Greater Mars-Ursa area, which represents a small part of the survey, the structures that were revealed in other areas are no less spectacular. Steep flanks, complex thrusts, vertical welds, and the basement reflector can now be reliably mapped. Furthermore, the FWI velocity model derived from geophysical first principles can now

become an interpretation-worthy product. For example, high-fidelity velocities may reveal areas of likely high/low pressures and help us understand the rock properties that are key to economically producible hydrocarbon-bearing reservoirs. The FWI velocity model also sheds light on intrasalt velocity variations within salt bodies, which in the past were modeled with either constant velocities or unreliable dirty salt velocity approximations. As the Venus salt example demonstrates, FWI velocity captures the physically meaningful subtle velocity variation within salt bodies, which impeded subsalt focusing. The high-fidelity FWI intrasalt velocity fields can now fully replace the dirty salt velocities derived from either limited intrasalt reflectivity data or traveltime tomography. Understanding the factors driving intrasalt velocity variability may shed additional light on salt tectonics history and the role salt may play in hydrocarbon migration.

Finally, one could argue that the current survey has derisked the new-generation exploration acquisition design for use in other parts of the Gulf of Mexico (GoM). Large parts of the GoM remain significantly underexplored due to the particularly challenging combination of salt canopy, uncalibrated sediment velocities, and resulting poor seismic image quality obtained with the previous generation of acquisition designs and velocity models. These new-generation surveys could unlock such underexplored GoM areas for active prospecting. ■■

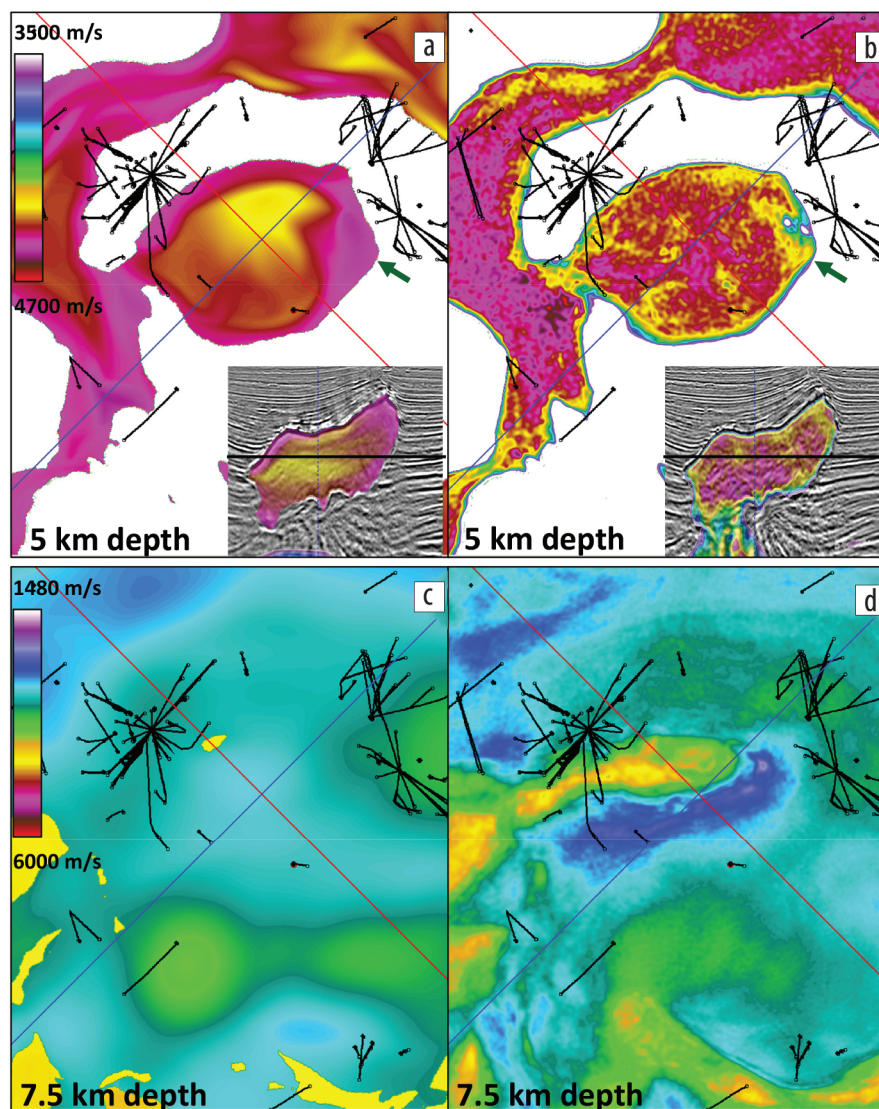


Figure 5. Comparison of velocity model depth slices at 5 and 7.5 km through the Venus salt. (a) and (c) 2016 dual-WAZ-based model. (b) and (d) Long-offset OBN-based FWI model. The color range in (a) and (b) is restricted to highlight velocity variation inside salt. The seismic insets in (a) and (b) show the OBN RTM image for the respective velocity model along the red inline, with the intrasalt velocities displayed on top. The dark green arrows in (a) and (b) indicate the area of the significant intrasalt velocity slowdown after FWI.

Acknowledgments

Many individuals have contributed to the project via inspiration, valuable ideas, suggestions, etc. In particular, some of the early passionate champions for a new-generation survey in the Greater Mars-Ursa area were Toby Perry and Jim Clippard, who are now retired from Shell. Other notable Shell contributors to the project were Hamish Macintyre, Jim Pickens, Wences Gouveia, Michael Kiehn, Fons ten Kroode, Michael Merritt, John Keating, Jeff Durand, Doug Rodenberger, and Tara Brothers. The TGS team included Duncan Bate, Terry Johnson, Carsten Udengaard, Raheel Malik, Linda Santiago, Yi Xuan, Eric Camarda, Hao Xing, and Gan Yu. We acknowledge Maisha Amaru and an anonymous reviewer for their comments that improved the article during the review stage. We thank TGS and partner WesternGeco for permission to publish data and results from the Freedom and Patriot WAZ and Amendment OBN surveys. Finally, we thank TGS, WesternGeco, and the clients' management for funding the survey.

Data and materials availability

Data associated with this research are confidential and cannot be released.

Corresponding author: daniel.chaikin@tgs.com

References

- Dellinger, J., A. Ross, D. Meaux, A. Brenders, G. Gesoff, J. Etgen, J. Naranjo, G. Openshaw, and M. Harper, 2016, Wolfspar[®], an "FWI-friendly" ultralow-frequency marine seismic source: 86th Annual International Meeting, SEG, Expanded Abstracts, 4891–4895, <https://doi.org/10.1190/segam2016-13762702.1>.
- Elebiju, B., K. Pratt, W. Gou, and Y. Zeng, 2016, Improving subsalt image from multiazimuth TTI reprocessing at Kepler Field, Gulf of Mexico: 86th Annual International Meeting, SEG, Expanded Abstracts, 5244–5248, <https://doi.org/10.1190/segam2016-13869411.1>.
- Huang, Y., J. Mao, C. Zeng, and J. Sheng, 2019, FWI salt model update trials with sparse nodes: 89th Annual International Meeting, SEG, Expanded Abstracts, 1255–1259, <https://doi.org/10.1190/segam2019-3215169.1>.
- Mao, J., J. Sheng, Y. Huang, F. Hao, and F. Liu, 2020, Multi-channel dynamic matching full-waveform inversion: 90th Annual International Meeting, SEG, Expanded Abstracts, 666–670, <https://doi.org/10.1190/segam2020-3427610.1>.
- Mei, J., Z. Zhang, F. Lin, R. Huang, P. Wang, and C. Miffin, 2019, Sparse nodes for velocity: Learnings from Atlantis OBN full-waveform inversion test: 89th Annual International Meeting, SEG, Expanded Abstracts, 167–171, <https://doi.org/10.1190/segam2019-3215208.1>.
- Nolte, B., F. Rollins, Q. Li, S. Dadi, S. Yang, J. Mei, and R. Huang, 2019, Salt velocity model building with FWI on OBN data: Example from Mad Dog, Gulf of Mexico: 89th Annual International Meeting, SEG, Expanded Abstracts, 1275–1279, <https://doi.org/10.1190/segam2019-3216777.1>.
- Priest, T., 2019, Shell Oil's deepwater mission to Mars, <https://dps.lib.uiowa.edu/mars-deepwater-gulf/history/>, accessed 5 October 2020.
- Roende, H., J. Sheng, Z. Liu, and D. Bate, 2019, Considerations for a model building paradigm shift in the Gulf of Mexico: 81st Conference and Exhibition, EAGE, Extended Abstracts, <https://doi.org/10.3997/2214-4609.201901406>.
- Roende, H., D. Bate, J. Mao, Y. Huang, and D. Chaikin, 2020, New node acquisition design delivers unprecedented results with dynamic matching FWI — Case study from the Gulf of Mexico: First Break, **38**, no. 9, 73–78, <https://doi.org/10.3997/1365-2397.fb2020068>.
- Shen, X., I. Ahmed, A. Brenders, J. Dellinger, J. Etgen, and S. Mitchell, 2017, Salt model building at Atlantis with full-waveform inversion: 87th Annual International Meeting, SEG, Expanded Abstracts, 1507–1511, <https://doi.org/10.1190/segam2017-17738630.1>.
- Van Avendonk, H., G. L. Christeson, I. O. Norton, and D. R. Eddy, 2015, Continental rifting and sediment infill in the northwestern Gulf of Mexico: *Geology*, **43**, no. 7, 631–634, <https://doi.org/10.1130/G36798.1>.
- Zhang, Z., J. Mei, F. Lin, R. Huang, and P. Wang, 2018, Correcting for salt misinterpretation with full-waveform inversion: 88th Annual International Meeting, SEG, Expanded Abstracts, 1143–1147, <https://doi.org/10.1190/segam2018-2997711.1>.